

# Improved measurements of $\chi_{cJ} \rightarrow$ $\Sigma^+ \bar{\Sigma}^-$ and $\Sigma^0 \bar{\Sigma}^0$ decays

Phys. Rev. D 97, 052011 (2018)

**Gu Shan**

**2018.11.23**

**JC 86 report**

# Introduction

- Experimental studies of charmonium decays can test calculations in quantum chromodynamics (QCD) and QCD based effective field theories.
- There are large differences between predictions and the experimental measurements, the branching fractions (BF) of  $\chi_{c0} \rightarrow \Sigma^+ \bar{\Sigma}^-$  and  $\Sigma^0 \bar{\Sigma}^0$  decays as measured by CLEO-c and BESIII are observed to violate the helicity selection rule from perturbative QCD (pQCD) and also do not agree with models based on the charm meson loop mechanism .
- Tests of the color octet mechanism (COM )using more decay channels are an important input for the development of the theoretical models

# Event topology

$$\mathbf{1}, \psi(3686) \rightarrow \gamma \chi_{cJ}, \chi_{cJ} \rightarrow \begin{matrix} \Uparrow \bar{p} \pi^0 \\ \Sigma^+ \bar{\Sigma}^- \\ \Downarrow p \pi^0 \end{matrix}$$

➤ Final states of signal:  $5\gamma p \bar{p}$ .

$$\mathbf{2}, \psi(3686) \rightarrow \gamma \chi_{cJ}, \chi_{cJ} \rightarrow \begin{matrix} \Uparrow \bar{p} \pi^+ \\ \Uparrow \gamma \bar{\Lambda} \\ \Sigma^0 \bar{\Sigma}^0 \\ \Downarrow \gamma \Lambda \\ \Downarrow p \pi^- \end{matrix}$$

➤ Final states of signal:  $3\gamma p \bar{p} \pi^+ \pi^-$ .

# Event Selection

## Channel 1:

select  $\pi^0, \Sigma^+, \bar{\Sigma}^-$

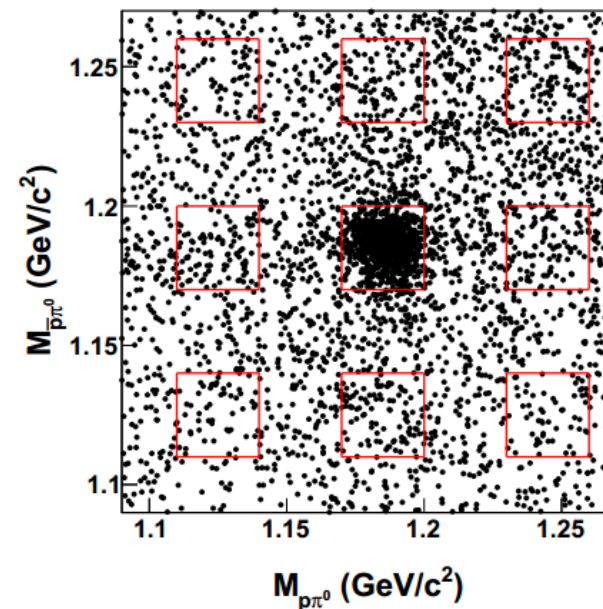
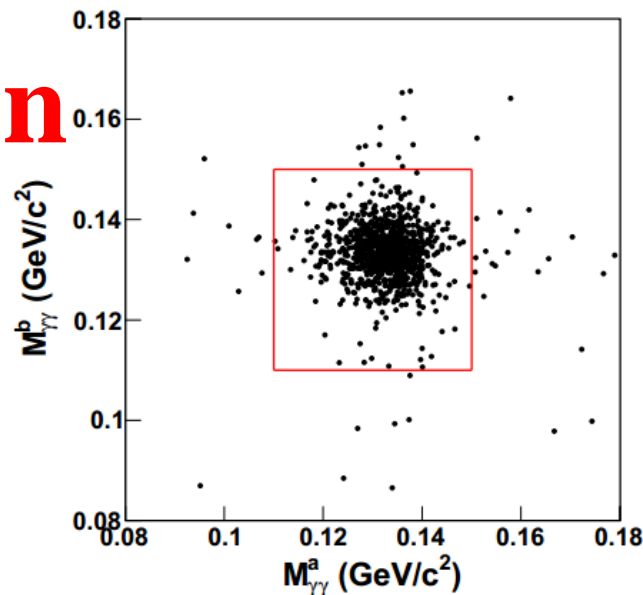


Fig. 1: Distribution of  $M_{\gamma\gamma}^a$  versus  $M_{\gamma\gamma}^b$  (left) and distribution of  $M_{p\pi^0}$  versus  $M_{\bar{p}\pi^0}$  (right) for  $\chi_{cJ} \rightarrow \Sigma^+ \bar{\Sigma}^-$ . The central (surrounding) boxes indicate the signal (sideband) regions.

## Channel 2:

select  $\Lambda, \bar{\Lambda}, \Sigma^0, \bar{\Sigma}^0$

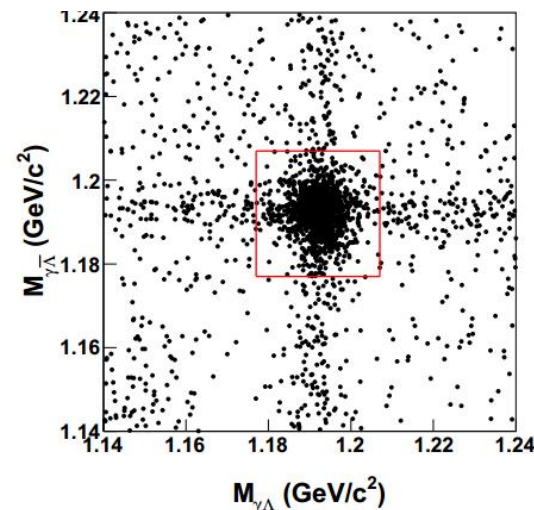
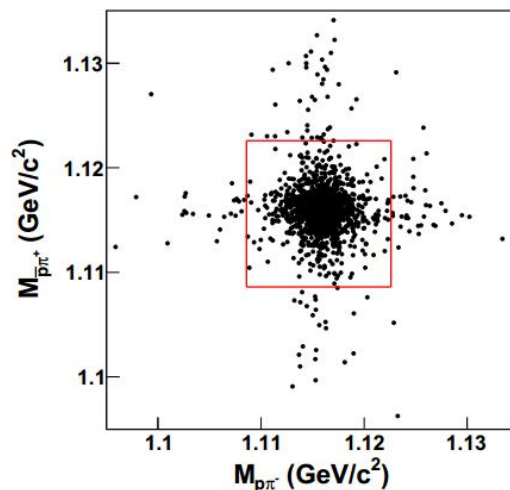


Fig. 3: Distribution of  $M_{p\pi^-}$  versus  $M_{\bar{p}\pi^+}$  (left) and distribution of  $M_{\gamma\Lambda}$  versus  $M_{\gamma\bar{\Lambda}}$  (right) for  $\chi_{cJ} \rightarrow \Sigma^0 \bar{\Sigma}^0$ . The solid boxes indicate the signal regions.

# Determination of the $\chi_{cJ}$ signals

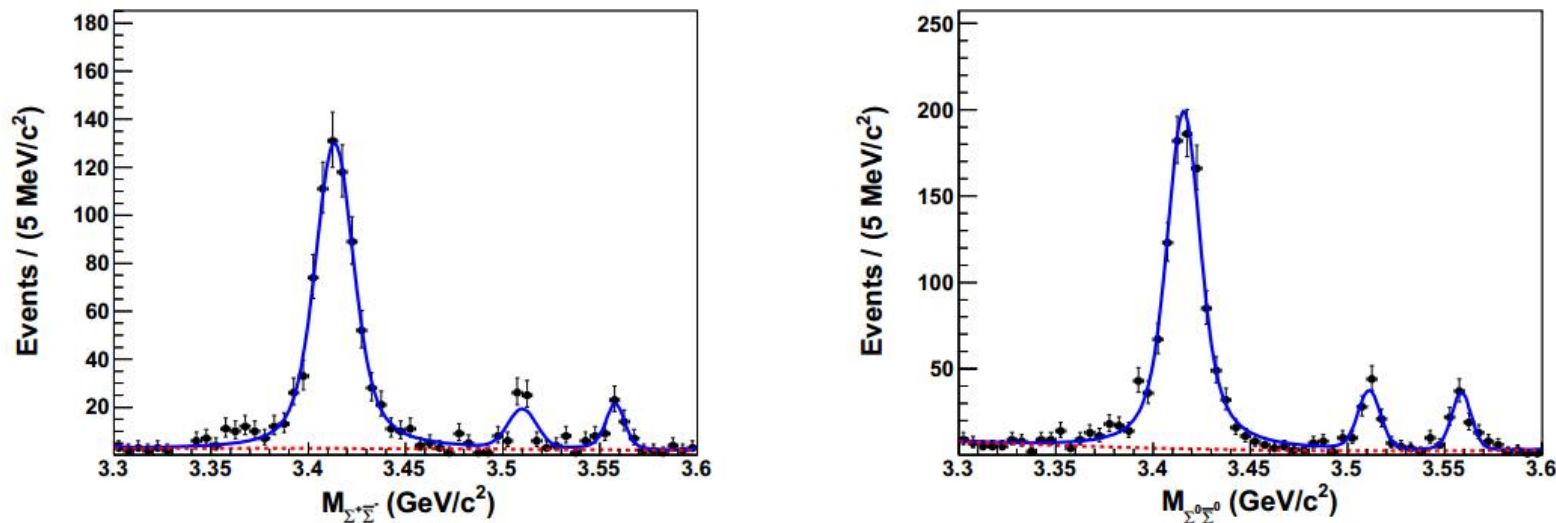


Fig. 4: Fit results to the invariant mass spectra of  $\Sigma^+\bar{\Sigma}^-$  (left) and  $\Sigma^0\bar{\Sigma}^0$  (right). The dots with error bars represent the data, the solid line represents the fit results and the dashed line represents the smooth background.

$$F_J(m) = (BW_J(m) \times E_\gamma^3 \times D(E_\gamma)) \otimes G(0; \sigma_{\text{res},J}),$$

where  $BW_J(m)$  is a Breit-Wigner function;  $G(0; \sigma_{\text{res},J})$  is a Gaussian function with the mean value of zero and a standard deviation of the detection resolution  $\sigma_{\text{res},J}$ ;  $E_\gamma^3$  is the cube of radiative photon energy reflecting the energy dependence of the electric dipole (E1) matrix element;  $D(E_\gamma)$  is a damping factor needed to suppress the diverging tail caused by the  $E_\gamma^3$  dependence and is given by  $e^{-\frac{E_\gamma^2}{8\beta^2}}$ , with  $\beta = 65$  MeV as determined by the CLEO collaboration [20]. The background is described by a second-order Chebychev polynomial function. In

# Result

TABLE II: The BF results for the measurement of  $\chi_{cJ} \rightarrow \Sigma^+ \bar{\Sigma}^-$  and  $\Sigma^0 \bar{\Sigma}^0$  (second column), together with values from PDG world average [17], previous measurement from BESIII publications [6], CLEO [5] and theoretical predictions [2–4] for comparison. To make an objective comparison, the BF of  $\chi_{cJ} \rightarrow \Sigma \bar{\Sigma}$  decays from previous BESIII are corrected with the newest BF of  $\psi(3686) \rightarrow \gamma \chi_{cJ}$  from Ref. [17]. To be independent of the BF of  $\psi(3686) \rightarrow \gamma \chi_{cJ}$ , the product BF ( $\mathcal{B}_{\text{prod}}$ ) of  $\psi(3686) \rightarrow \gamma \chi_{cJ}$  and  $\chi_{cJ} \rightarrow \Sigma \bar{\Sigma}$  are also listed (last column). The first uncertainty is statistical and the second systematic. Throughout the table, the BFs are given in units of  $10^{-5}$ .

Channel	This work	PDG	Previous BESIII [6]	CLEO [5]	Theory	$\mathcal{B}_{\text{prod}}$
$\chi_{c0} \rightarrow \Sigma^+ \bar{\Sigma}^-$	$50.4 \pm 2.5 \pm 2.7$	$39 \pm 7$	$43.7 \pm 4.0 \pm 2.8$	$32.5 \pm 5.7 \pm 4.3$	5.5-6.9 [3]	$4.99 \pm 0.24 \pm 0.24$
$\chi_{c1} \rightarrow \Sigma^+ \bar{\Sigma}^-$	$3.7 \pm 0.6 \pm 0.2$	$< 6$	$5.2 \pm 1.3 \pm 0.5 (< 8.3)$	$< 6.5$	3.3 [4]	$0.35 \pm 0.06 \pm 0.02$
$\chi_{c2} \rightarrow \Sigma^+ \bar{\Sigma}^-$	$3.5 \pm 0.7 \pm 0.3$	$< 7$	$4.7 \pm 1.8 \pm 0.7 (< 8.4)$	$< 6.7$	5.0 [4]	$0.32 \pm 0.06 \pm 0.03$
$\chi_{c0} \rightarrow \Sigma^0 \bar{\Sigma}^0$	$47.7 \pm 1.8 \pm 3.5$	$44 \pm 4$	$46.0 \pm 3.3 \pm 3.7$	$44.1 \pm 5.6 \pm 4.7$	$(25.1 \pm 3.4, 18.7 \pm 4.5)$ [2]	$4.72 \pm 0.18 \pm 0.28$
$\chi_{c1} \rightarrow \Sigma^0 \bar{\Sigma}^0$	$4.3 \pm 0.5 \pm 0.3$	$< 4$	$3.7 \pm 1.0 \pm 0.5 (< 6.0)$	$< 4.4$	3.3 [4]	$0.41 \pm 0.05 \pm 0.03$
$\chi_{c2} \rightarrow \Sigma^0 \bar{\Sigma}^0$	$3.9 \pm 0.5 \pm 0.3$	$< 6$	$3.8 \pm 1.0 \pm 0.5 (< 6.2)$	$< 7.5$	$(38.9 \pm 8.8, 4.2 \pm 0.5)$ [2] 5.0 [4]	$0.35 \pm 0.05 \pm 0.02$

Overall, we have measured the BF of  $\chi_{cJ} \rightarrow \Sigma \bar{\Sigma}$  and  $\Sigma^0 \bar{\Sigma}^0$ . The results presented replace the previous BESIII results [6]. The decays  $\chi_{c1,2} \rightarrow \Sigma^+ \bar{\Sigma}^-$  and  $\Sigma^0 \bar{\Sigma}^0$  are observed with more than  $5\sigma$  significance for the first time. The results are consistent with and improve on the precision compared to the world average values. The current results on  $\chi_{c1,2} \rightarrow \Sigma^+ \bar{\Sigma}^-$  and  $\Sigma^0 \bar{\Sigma}^0$  are in good agreement with theoretical predictions based on the color octet contribution model [4]. The results for  $\chi_{c0} \rightarrow \Sigma^+ \bar{\Sigma}^-$  and  $\Sigma^0 \bar{\Sigma}^0$  are still inconsistent with the prediction [3] based on the charm meson loop mechanism. The ratio between charged and neutral decay modes is consistent with the expectation from isospin symmetry.

## Question from Xin

Could you briefly explain what is the “color octet mechanism (OCM)” ? Probably with Feynman diagram ...

**Answer:** It's a model in the Non-relativistic Quantum Chromodynamics, (NRQCD), it is used to deal with the decay of the colored heavy quark-antiquark pairs on the short and long distance scale problem.

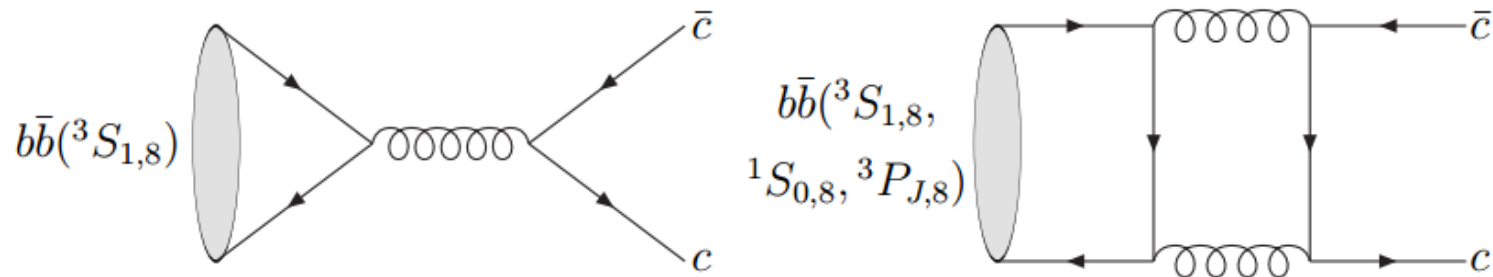


图 5.2 色八重态的  $b\bar{b} \rightarrow c\bar{c}$  的费曼图



- **Question from AMIT**

- Can you please explain what is Helicity Selection Rule with a suitable example?

- **Answer:**

We briefly review this powerful method that is elaborated on in Ref. [2]. For a charmonium meson  $J_{c\bar{c}}$  decaying into two light mesons  $h_1$  and  $h_2$ , the perturbative method gives the asymptotic behavior of the branching ratio as follows

$$BR_{J_{c\bar{c}}(\lambda) \rightarrow h_1(\lambda_1)h_2(\lambda_2)} \sim \left( \frac{\Lambda_{QCD}^2}{m_c^2} \right)^{|\lambda_1 + \lambda_2| + 2}, \quad (1)$$

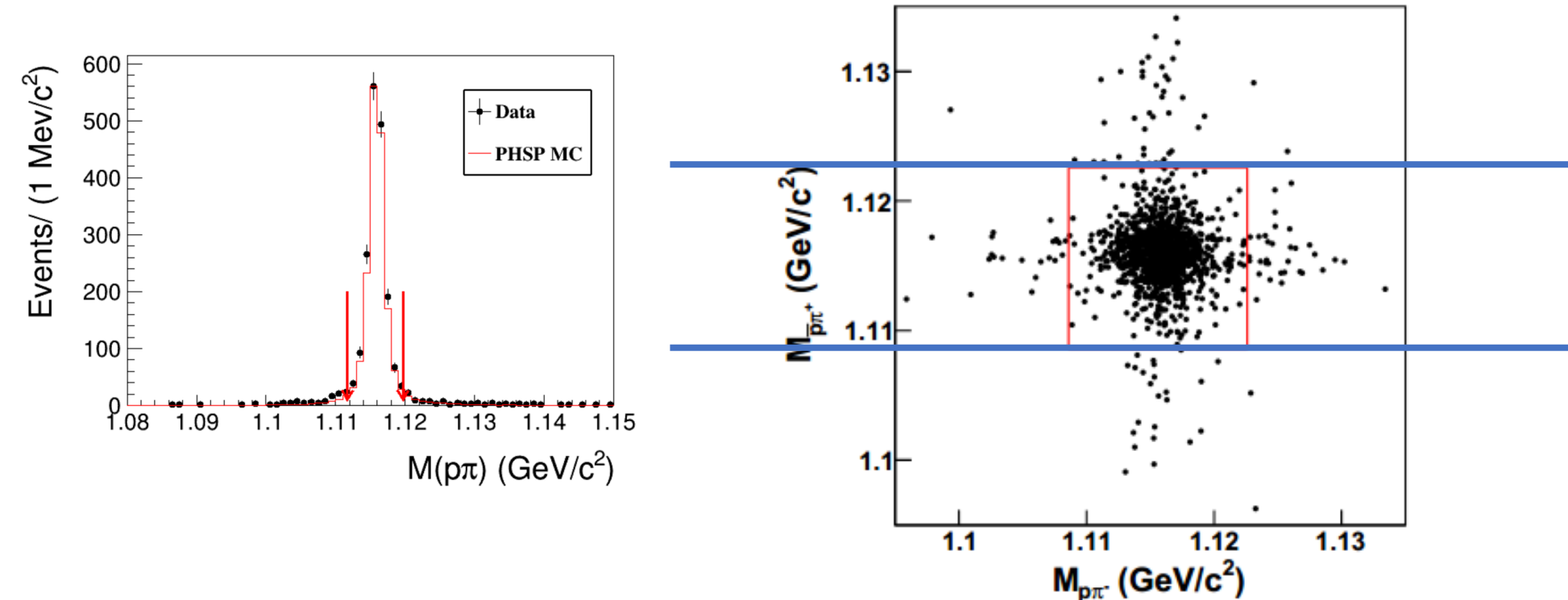
where  $\lambda$ ,  $\lambda_1$ , and  $\lambda_2$  are the helicities of the corresponding mesons. This is the result of the pQCD method to leading-twist accuracy; i.e. only the valence Fock state (here it is  $c\bar{c}$ ) is considered. It is obvious that the leading contribution comes from when  $\lambda_1 + \lambda_2 = 0$ , (while the higher twist will be suppressed by at least a factor of  $\Lambda_{QCD}^2/m_c^2$ .) while the helicity configurations which do not satisfy this relation will be suppressed.



## Question from Yuzhen

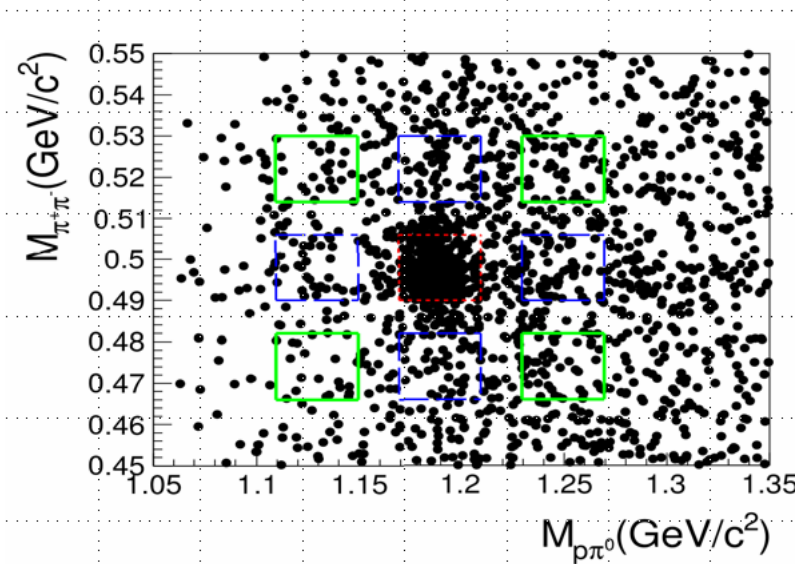
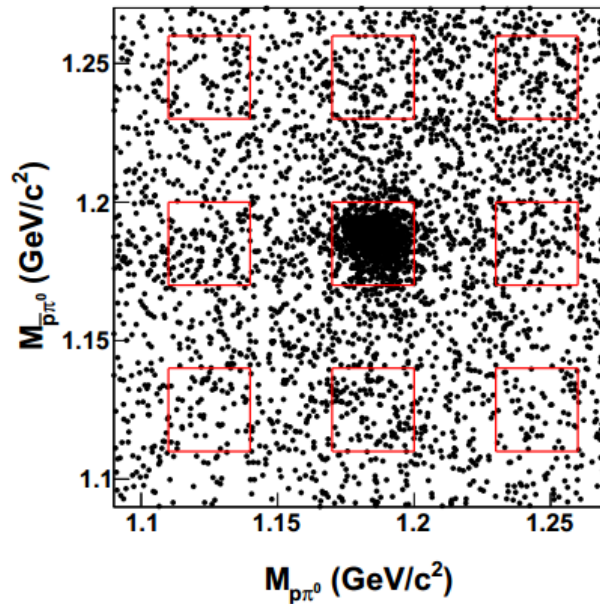
- In Fig.3 (left), the density of black point in the center is highest, but density of up, underneath, left and right side of the center is a little higher than other places, why?

**Answer:**1, He has selected the clean  $\Lambda$  signals.  
2, The width of  $\Lambda$  is very narrow.

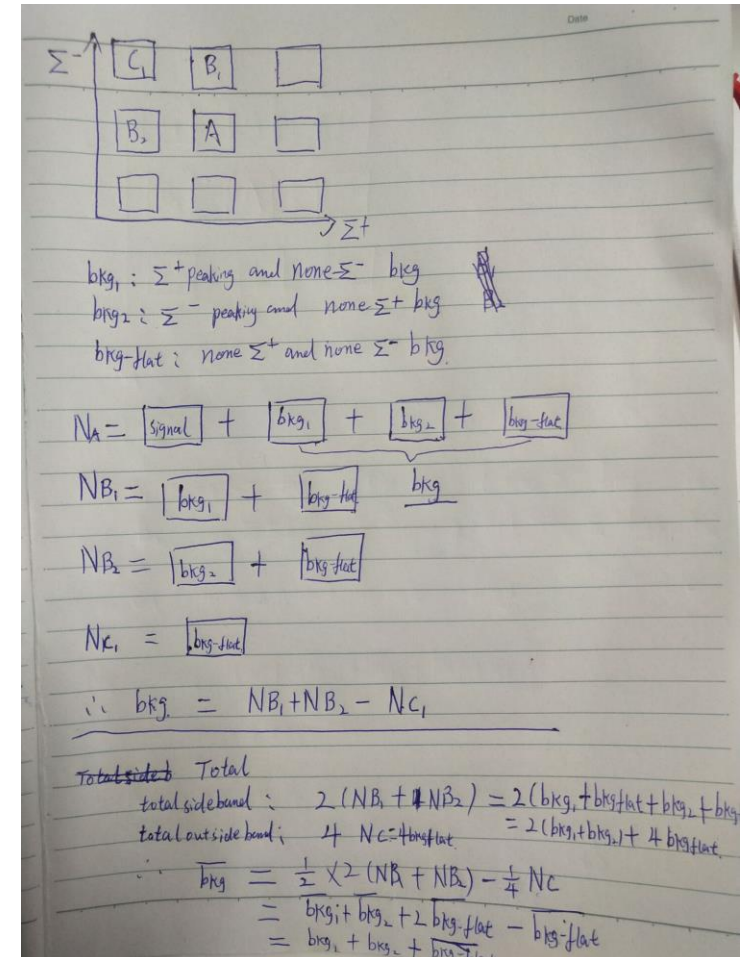


## • Question from Suyu

- In right panel of figure 1, what's the rule to select such the boxes as background? As I remember, you did some similar thing in your analysis. Why some box contributes as 1/4 while others 1/2?



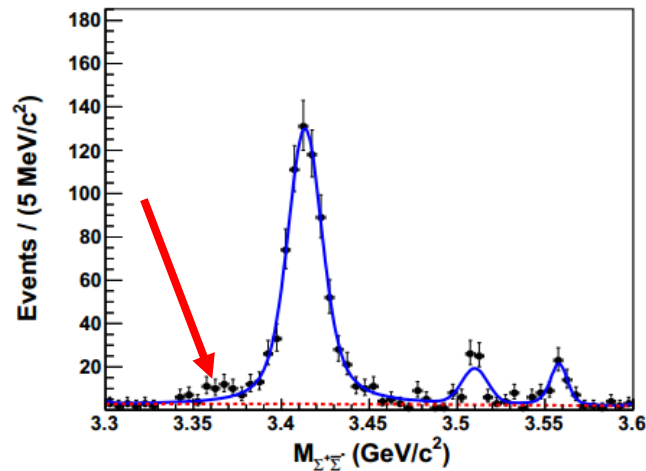
$$N_{\text{bkg}} = \frac{1}{2} N_{\text{blue}} - \frac{1}{4} N_{\text{green}}$$



- **Question from Kai**
- section V, the PDF of signal peaks including a Gaussian function, why the mean value is set to be zero?
- **Answer:** Actually, if we didn't set it to be zero, the mean of the shape will shift because of the convolution. Usually we will set it to 0. otherwise it will give a very small change interval.

- **Question from Ryuta**

- In the Fig.4 (left), the invariant mass of Sigma<sup>+</sup>/Sigma<sup>-</sup>, I could find a small bump-like structure around 3.36-3.37 GeV. If I check that for the case of Sigma<sup>+</sup>/Pbar/K<sup>0</sup>short, as you have shown last week, there also would be a similar structure on this region.
- Is there any internal discussion on this structure (possibly some background ?) or not ?
- **Answer:** No discussion on this.



- **Question from Yuhang**

- In TABLE II, the theoretical value is far from the measured value in  $\chi_{c0} \rightarrow \Sigma^+ \Sigma^-$  channel. In summary, it also says: “The results for  $\chi_{c0} \rightarrow \Sigma^+ \Sigma^-$  and  $\chi_{c0} \rightarrow \Sigma^0 \Sigma^0$  are still inconsistent with the prediction.” What caused this result?
- **Answer:**  $\chi_{c0} \rightarrow \Sigma \bar{\Sigma}$  is supposed to be highly suppressed by the helicity selection rule. However, J. Phys. G 38, 035007 (2011) results indicate that the transitions via these kinds of loops as long-distance effects can give **significant contributions**. This is a further test of the mechanism for the evasion of helicity selection rule that proposed in Phys. Rev. D 81, 014017 (2010).

Here, the result from experiment is more bigger than the result from the J. Phys. G 38, 035007 (2011) prediction. So maybe theorists can propose more models or explanations. (I don't know.....)